297

Kinematic of 3-wheels swerve drive using BLDC motor

Arif Anwar Rosyidin[1], Indrazno Siradjuddin[1], Ratna Ika Putri[1], Mas Nurul Achmadiah[*1]
State Polytechnic of Malang, Indonesia[1]

Abstract
The stability of the robot's performance is very important, especially for the wheeled mobile robots that use swerve drives, which need kinematic control to reach the destination point. The study of robot movement known as kinematics is based on an examination of the geometric structure of the robot, with no consideration given to the mass, force, or acceleration that the robot experiences during movement. This study aims to model and simulate the kinematic control design of a wheeled robot that uses a swerve drive. This robot uses BLDC motor actuator so that the robot can reach its destination very quickly and steadily. The test is carried out by simulating and comparing the performance response using BLDC motors and DC motors. According to the testing and trials, the robot can reach its destination by modeling its kinematic control, and BLDC motors are found to be more reliable and efficient for driving and steering than DC motors.

1. Introduction

Wheeled mobile robots are one example of how science and technology have profoundly changed human life [1], [2]. Wheeled mobile robots are utilized for essential missions and a variety of tasks since they have a high degree of maneuverability [3]. This type of robot can be used as the basis for other independent robots or be equipped with an arm or other robot according to the needs. Wheeled robot technology has recently advanced, opening up a wide range of applications in the medical, hospital, industrial, and warehousing spaces [4], [5]. Based on the movement and Degree of Freedom, the wheeled mobile robot is divided into two, namely holonomic and non-holonomic. Non-holonomic robots cannot change their position instantly or quickly. Holonomic robots are robots that can change positions quickly or instantly [6], [7]. The examples of holonomic robots are omnidirectional, swerve drive, and others. The swerve drive system is usually called independent driving and independent steering [8], [9]. Swerve drive has 2 motors, namely for driving and for steering. The benefit of swerve drive is that it allows for a slight amount of wheel slippage, which enhances the robot's performance and increases its mobility since the wheels may concurrently conduct translational and rotational motions.

Wheeled mobile robot control and stability are important in the field of robotics [10], [11]. Motion control is the core problem in wheeled robot systems that ensures smooth robot movement [12]. There are two different types of issues with mobile robots: systematic errors and non-systematic errors. The robot system's inaccuracies lead to systematic errors. Roads, outside disturbances, and alterations in the environment are examples of external disturbances that contribute to non-systematic errors. However, the major problem with this kind of application is one of the systematic errors, i.e., movement, which therefore, requires kinematic. The kinematic model is as fundamental as manipulator to a Wheeled Mobile Robot (WMR) [13]. Kinematics calculations depend on the robot's specifications, including the number of actuators used to control speed and wheel steering. The WMR kinematic model specifies the geometry of the WMR without taking into account the mass, inertia, or the coefficient of friction at the wheels. It also defines the limits between the position and velocity of the WMR body, wheels, and steering linkages [14]. The Kinematic on the mobile robot is divided into two, namely forward kinematic and inverse kinematic [1], [13]. Forward kinematics uses each wheel's angular velocity to determine the WMR's location and orientation. The angular velocity is determined via inverse kinematics using the position and orientation of the WMR [15].

In this study, a BLDC motor is used. The BLDC motor was chosen because it has several advantages compared to DC motors and can speed up the robot reaching the destination point. There are several advantages of using a BLDC motor: high efficiency, high speed, small noise, rarely repaired, and easy to control [16], [17], [18]. BLDC motors are actually PMSM but they use a trapezoidal shape in the back-EMF signal [19]. BLDC motors are almost the same as DC motors, the difference is the commutation system. BLDC motors use an electric commutation system while DC motors

are still mechanical. Set the commutation system required an inverter [20]. The BLDC motor stator will receive the DC power source once it passes through the inverter. Since the rotor's location is also a basis for the commutation system, locating the rotor requires the use of a position sensor. A hall sensor is used by BLDC motors to detect the rotor's location [21].

This article is divided into several parts, namely the first section containing rigid body motion, the second section containing kinematic modeling of 3-wheel swerve drive, the third section containing mathematical modeling of BLDC motors, the fourth section presenting the simulation results of 3-wheel swerve drive using BLDC motors, and the last section is the conclusion of this article.

2. Research Method

This chapter describes the rigid body, kinematic modeling of the 3-wheel swerve drive, and mathematical modeling of the BLDC motor.

2.1 Rigid Body Motion

Robot kinematics development starts with the idea of rigid body motion, emphasizing its geometrical characteristics. Rigid body motion consists of translational and rotational motion.
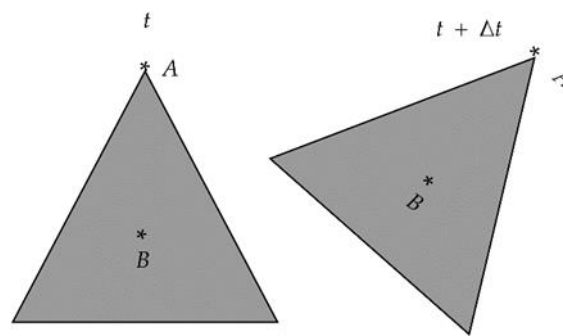

Figure 1. Robot Motion at 2D

Figure 1 is the movement of the robot body from the t time to the $t + \Delta t$. In Figure 1 it can be seen that there are 2 types of movements, namely translational and rotational movements. Translational motion is a displacement movement that changes the distance from the initial position without changing the facing direction and rotational motion is a rotational movement that does not change the distance but changes the facing direction which results in an angle from the initial condition. In Figure 1 there are 2 points whose positions are always fixed, namely A and B. the distance between points A and B can be denoted as $r_{A/B}$.
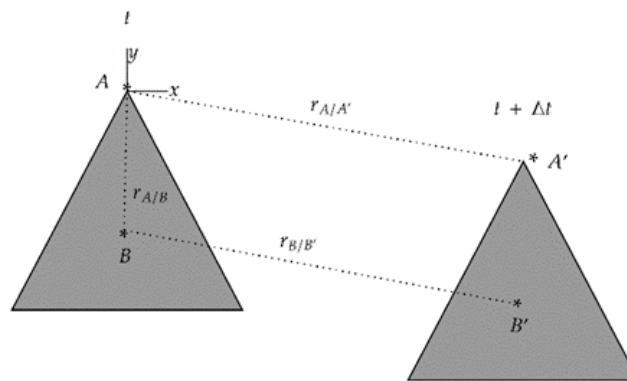

Figure 2. Translational Motion

Figure 2 is the translational movement of the robot. Because the robot changes places, points A and B also experience a move, point A to point A' and point B to point B'. Even though the robot changes places, the distances A and B remain the same. Therefore, it can be denoted as in Equation 1 and Equation 2.

$$r_{A/B} = r_{A'/B'} \tag{1}$$
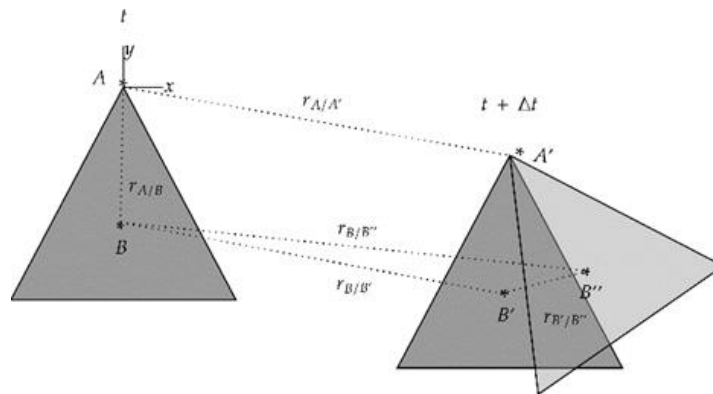
$$r_{A/A'} = r_{B/B'} \tag{2}$$

Figure 3. Rotational Motion

Then, in Figure 3, the robot experiences rotation after translation. The rigid body motion in this instance revolves around a fixed axis, specifically, the axis z, which is associated with point A' and an angular velocity of ω. In these conditions, the point B' changes position to B'' as far as $r_{B'/B''}$, the mathematical equation can be seen in Equation 3.

$$r_{B/B''} = r_{B/B'} + r_{B'/B''} \tag{3}$$

If Equation 3 is derived to time, the following mathematical form will be obtained as seen in Equation 4:

$$\frac{\mathrm{d}r_{B/B''}}{\mathrm{d}t} = \frac{\mathrm{d}r_{B/B'}}{\mathrm{d}t} + \frac{\mathrm{d}r_{B'/B''}}{\mathrm{d}t} \tag{4}$$

$$v_{B/B''} = v_{B/B'} + v_{B'/B''} \tag{5}$$

Equation 5 is an equation of the change in velocity with time. $v_{B/B'}$ is the speed of change of position from point B to point B', $v_{B/B''}$ is the speed of change of position from point B to point B'', and $v_{B'/B''}$ is the velocity of change of position from point B' to point B'' with reference to the axis of rotation at point A'. The notation $v_{B'/B''}$ equals the angular velocity (ω), the equation can be seen in Equation 6.

$$v_{B/B''} = v_{B/B'} + \omega \times r_{B'/B''} \tag{6}$$

2.2 Kinematic Modelling on 3-wheels swerve drive

The science of robot movement known as kinematic modeling is based on the examination of robot coordinates alone, without taking force, torque, or acceleration into account [22]. In this section, 3-wheels swerve drive structure model is described. The model is very important to determine the kinematic equation of the robot [23]. Figure 4 describes the model of 3-wheels swerve drive robot.
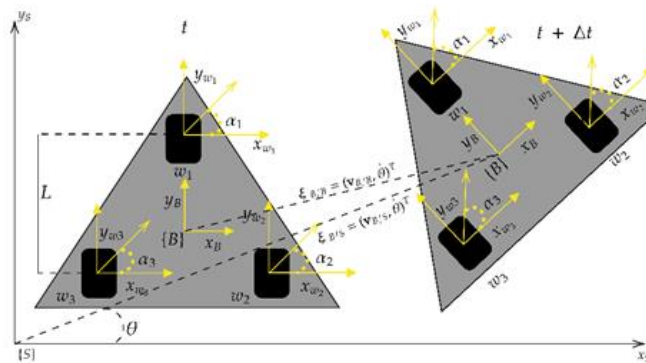

Figure 4. Motion of Swerve Robot 3 Wheels

Before we determine the movement, the coordinates (frames) that the robot may utilize as a reference while it is moving must be found [24]. The frame on the robot body is determined by taking the midpoint of the robot body which is denoted as (B) and the frame on the wheels is determined by taking the midpoint of each robot wheel which is denoted by (W_i). To control the speed of the robot body which is affected by the wheel rotational speed of the robot body itself is denoted as $(v_{W/B})$, the mathematical form can be seen in Equation 7.

$$v_{W/B} = v_{B/B} + \omega \times r_{W/B} \tag{7}$$

Where $\mathbf{v}_{W/B} = \left(x_{\dot{W}/B}, y_{\dot{W}/B}, z_{\dot{W}/B}\right)^\top$ s the speed of the wheel against the robot body and $\mathbf{v}_{B/B} = \left(x_{\dot{B}/B}, y_{\dot{B}/B}, z_{\dot{B}/B}\right)^\top$ is the speed of the body against the frame [25]. Because the angular speed of the robot is only on the Z axis, the ω value in the Equation 7 is this and the Equation 7 can be solved with the cross product so that it becomes the following as seen in Equation 8.

$$\begin{pmatrix} x_{\dot{W}/B} \\ y_{\dot{W}/B} \end{pmatrix} = \begin{pmatrix} x_{\dot{B}/B} \\ y_{\dot{B}/B} \end{pmatrix} + \begin{pmatrix} -y_{W_i}\omega_z \\ x_{W_i}\omega_z \end{pmatrix} \tag{8}$$

A homogeneous matrix is needed to calculate the robot's speed against the global frame as seen Equation 9, Equation 10, and Equation 11.

$$\boldsymbol{\xi}_{B/S} = H_{B/S} \quad \boldsymbol{\xi}_{B/B} \tag{1}$$

$$\boldsymbol{\xi}_{B/S} = \begin{pmatrix} \boldsymbol{R}_{B/S} & \boldsymbol{0} \\ \boldsymbol{0}^T & 1 \end{pmatrix} \begin{pmatrix} v_{B/B} \\ \omega_z \end{pmatrix} \tag{10}$$

$$\boldsymbol{\xi}_{B/S} = \underbrace{\begin{pmatrix} cos(\theta) & -sin(\theta) & 0 \\ sin(\theta) & cos(\theta) & 0 \\ 0 & 0 & 1 \end{pmatrix} \begin{pmatrix} \dot{x} \\ \dot{y} \\ \dot{\theta} \end{pmatrix}}_{\text{spatial twist velocity}} \tag{11}$$

Equation 11 is often called forward kinematic or spatial body velocity, θ is the angle that the robot has made based on the global frame, and ω_z is the angular velocity in the z-axis. Finding the inverse kinematic is the primary objective of kinematic modeling in order to enable the robot to travel at a specific wheel speed in the direction of a predefined location. The inverse kinematic or often called body twist velocity can be calculated by using Equation 12, Equation 13, and Equation 14.

$$\boldsymbol{\xi}_{B/B} = H_{B/S}^{-1} \quad \boldsymbol{\xi}_{B/S} \tag{12}$$

$$\boldsymbol{\xi}_{B/B} = \begin{pmatrix} \boldsymbol{R}^{-1}_{B/S} & \boldsymbol{0} \\ \boldsymbol{0}^T & 1 \end{pmatrix} \begin{pmatrix} v_{B/S} \\ \omega_z \end{pmatrix} \tag{13}$$

$$\boldsymbol{\xi}_{B/B} = \underbrace{\begin{pmatrix} cos(\theta) & sin(\theta) & 0 \\ -sin(\theta) & cos(\theta) & 0 \\ 0 & 0 & 1 \end{pmatrix} \begin{pmatrix} \dot{x} \\ \dot{y} \\ \dot{\theta} \end{pmatrix}}_{\text{body twist velocity}} \tag{14}$$

$$v_{W/B} = \boldsymbol{R}_{B/S}^{-1} v_{B/S} + \boldsymbol{\omega} \times \boldsymbol{r}_{W/B} \tag{15}$$

$$= \begin{pmatrix} cos(\theta) & sin(\theta) \\ -sin(\theta) & cos(\theta) \end{pmatrix} \begin{pmatrix} \dot{x} \\ \dot{y} \end{pmatrix} + \begin{pmatrix} -y_{W_i}\omega_z \\ x_{W_i}\omega_z \end{pmatrix} \tag{16}$$

Based on Equation 15 and Equation 16, to get the parameter Body Twist Velocity in total, it can be calculated using the following equation as seen in Equation 17.

$$v_{W/B} = \begin{pmatrix} 1 & 0 & -y_i \\ 0 & 1 & x_i \end{pmatrix} \begin{pmatrix} cos(\theta) & sin(\theta) & 0 \\ -sin(\theta) & cos(\theta) & 0 \\ 0 & 0 & 1 \end{pmatrix} \begin{pmatrix} \dot{x} \\ \dot{y} \\ \dot{\theta} \end{pmatrix} \tag{17}$$

Equation 17 is applied to control 1 wheel, so to control 3-wheels the equation is as seen in Equation 18.

$$\begin{bmatrix} \dot{x}_{w_1/B} \\ \dot{y}_{w_1/B} \\ \dot{x}_{w_2/B} \\ \dot{y}_{w_2/B} \\ \vdots \\ \dot{x}_{w_N/B} \\ \dot{y}_{w_N/B} \end{bmatrix} = \begin{bmatrix} 1 & 0 & -y_1 \\ 0 & 1 & x_1 \\ 1 & 0 & -y_2 \\ 0 & 1 & y_2 \\ \vdots & \vdots & \vdots \\ 1 & 0 & -y_N \\ 0 & 1 & x_N \end{bmatrix} H_{B/S}^{-1} \begin{bmatrix} \dot{x}_{B/S} \\ \dot{y}_{B/S} \\ \omega_z \end{bmatrix} \tag{18}$$

Based on Figure 4, to determine the position of each wheel, the width and length are divided into 2 so that it becomes as seen in Equation 19.

$$\begin{bmatrix} \dot{x}_{w_1/B} \\ \dot{y}_{w_1/B} \\ \dot{x}_{w_2/B} \\ \dot{y}_{w_2/B} \\ \dot{x}_{w_3/B} \\ \dot{y}_{w_3/B} \end{bmatrix} = \begin{bmatrix} 1 & 0 & 0 \\ 0 & 1 & L \\ 1 & 0 & \dfrac{L\sqrt{3}}{2} \\ 0 & 1 & \dfrac{L}{2} \\ 1 & 0 & -\dfrac{L\sqrt{3}}{2} \\ 0 & 1 & -\dfrac{L}{2} \end{bmatrix} H_{B/S}^{-1} \begin{bmatrix} \dot{x}_{B/S} \\ \dot{y}_{B/S} \\ \omega_z \end{bmatrix} \tag{19}$$

The translational wheel speed is, u_i., and the steering angle control is α_i. The equation is as seen in Equation 20 and Equation 21.

$$\boldsymbol{\alpha_i} = arctan \frac{\dot{y}_{wi}}{\dot{x}_{wi}} \tag{20}$$

$$\boldsymbol{u_i} = \sqrt{(\dot{x}_{wi})^2 + (\dot{y}_{wi})^2} \tag{21}$$

2.3 Mathematic Modelling of BLDC Motor

Based on Figure 5, we can determine the mathematical equations and see the behavior of the BLDC motor. In the mathematical modeling of BLDC motors, machine parameter assumptions include the induced current (I) and voltage (V) on the permanent magnet (PM) rotor side and the harmonics on the stator winding side. Additionally, stray and iron losses (Li and Ls, respectively) are disregarded [26]. So the mathematical modeling of bldc can be written as seen in Equation 22, Equation 23, Equation 24, and Equation 25.
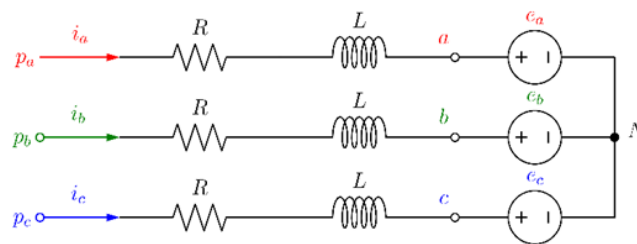

Figure 5. BLDC Motor Equivalent

$$v_{ab} = R(i_a - i_b) + L\frac{d}{dt}(i_a - i_b) + e_a - e_b \tag{22}$$

$$v_{bc} = R(i_b - i_c) + L\frac{d}{dt}(i_b - i_c) + e_b - e_c \tag{23}$$

$$v_{ca} = R(i_c - i_a) + L\frac{d}{dt}(i_c - i_a) + e_c - e_a \tag{24}$$

$$T_e = K_f \omega_m + J\frac{d\omega_m}{dt} + T_l \tag{25}$$

Where v,i, and e are denoted as phase voltage, phase current, and phase back-EMF. R and L are denoted as the resistance and inductance of each phase. T_e and T_L are denoted as the electric torque and the load torque. J is denoted as the rotor inertia, K_f is the friction constant, and ω_m is the rotor speed. Because the distance between the phases is 120 degrees, back-EMF and torque on bldc motors can be expressed as seen in Equation 26, Equation 27, Equation 28, and Equation 29.

$$e_a = \frac{K_e}{2}\omega_m F(\theta_e) \tag{26}$$

$$e_b = \frac{K_e}{2}\omega_m F\left(\theta_e - \frac{2\pi}{3}\right) \tag{27}$$

$$e_c = \frac{K_e}{2}\omega_m F\left(\theta_e - \frac{4\pi}{3}\right) \tag{28}$$

$$T_e = \frac{K_t}{2}\left(F(\theta_e)i_a + F\left(\theta_e - \frac{2\pi}{3}\right)i_b + F\left(\theta_e - \frac{4\pi}{3}\right)i_c\right) \tag{29}$$

Where K_e and K_t are back emf constants and torque constants for BLDC motors. θ_e is electrical angle or equal mechanical angle times number of pole $\theta_e = \frac{P}{2}\theta_m$. F is a function of the trapezoidal or sinusoidal waveform of back-EMF's BLDC motor [27].

$$\frac{dI_a}{dt} = -\frac{3RI_a}{L} - \frac{2E_a}{3L} + \frac{E_b}{3L} + \frac{E_c}{3L} + \frac{2V_a}{3L} - \frac{V_b}{3L} - \frac{V_c}{3L} \tag{30}$$

$$\frac{dI_b}{dt} = -\frac{3RI_b}{L} + \frac{E_a}{3L} - \frac{2E_b}{3L} + \frac{E_c}{3L} - \frac{V_a}{3L} + \frac{2V_b}{3L} - \frac{V_c}{3L} \tag{31}$$

$$\frac{d\omega_m}{dt} = -\frac{\beta\omega_m}{J} + \frac{T_e - T_i}{J} \tag{32}$$

$$\frac{d\theta_m}{dt} = \omega_m \tag{33}$$

and based on Equation 30, Equation 31, Equation 32, and Equation 33, the state space model is obtained which is shown in Equation 34:

$$\begin{bmatrix} i_a \\ i_b \\ \omega_m \\ \theta_m \end{bmatrix} = \begin{bmatrix} -\frac{R_a}{L_a} & 0 & 0 & 0 \\ 0 & -\frac{R_a}{L_a} & 0 & 0 \\ 0 & 0 & \frac{-b}{J} & 0 \\ 0 & 0 & 1 & 0 \end{bmatrix} \begin{bmatrix} i_a \\ i_b \\ \omega_m \\ \theta_m \end{bmatrix} + \begin{bmatrix} \frac{2}{3L_a} & \frac{2}{3L_a} & 0 \\ -\frac{2}{3L_a} & \frac{2}{3L_a} & 0 \\ 0 & 0 & \frac{1}{J} \\ 0 & 0 & 0 \end{bmatrix} \begin{bmatrix} V_{ab} - E_{ab} \\ V_{bc} - E_{bc} \\ T_e - T_L \end{bmatrix} \tag{34}$$

3. Result and Discussion

The robot will move toward the desired point. The robot's starting location is $(x, y, \theta)^\top = (0m, 0m, 0°)^\top$ then the robot will move towards the point $(x^*, y^*, \theta^*)^\top = (5m, 10m, 180°)^\top$ and compare the performance of swerve drives using BLDC and DC motors. The BLDC motor's specifications are listed in this article [28]. The parameters of the DC motor used follow this article [29]. The following is the result of the simulation.

3.1 Simulation kinematic of 3-wheels swerve drive using BLDC motor

Considering the outcomes found in Figure 6(a), the robot starts moving from the initial coordinates (green arrow direction), namely (0,0) in the facing direction 0° to the destination point (black arrow direction), namely (10,10) in the facing direction 180°, showing within 7 seconds the robot has arrived at the destination point, Figure 6(b) provides the evidence of this, showing that the robot may halt at the target when the error number reaches 0. This means that the kinematic control has worked as desired when using the BLDC motor. This is also evident in Figure 7(a) which is the speed response of each wheel, the speed response of each wheel can be seen at the beginning of the robot moving the speed of each wheel is very high but when it reaches the destination the speed will decrease until it reaches 0 rpm

or the motor stops moving. Figure 7(b) shows where each wheel is located. When the robot reaches the required angle, its wheel position will either remain constant or shift at the beginning of its movement.
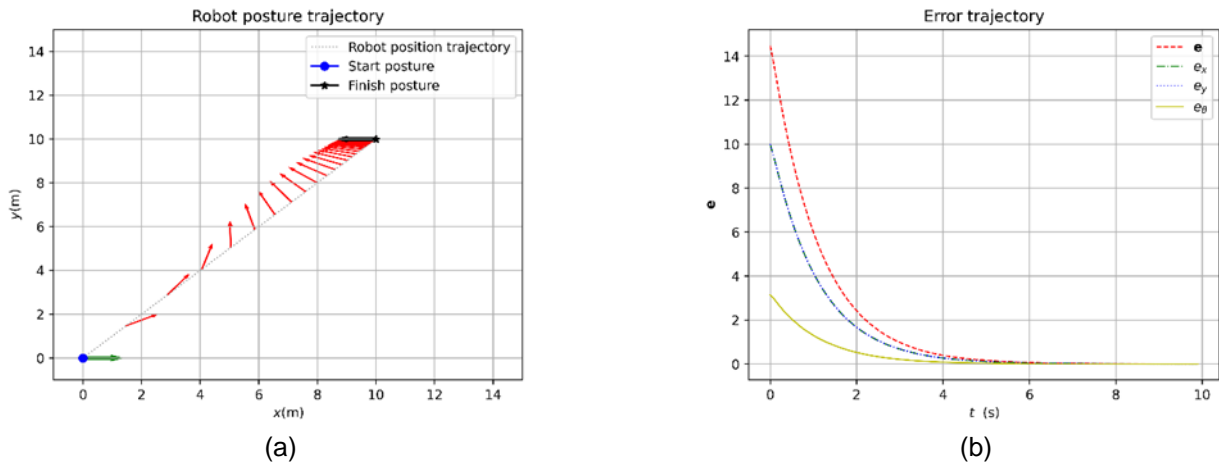

(a)   (b)

Figure 6. (a) Body Posture Robot using BLDC Motor, (b) Error Trajectory using BLDC Motor

Based on Figure 6(b) and Figure 7(a), the use of BLDC motors in driving can accelerate the robot to reach a predetermined point. The speed of the BLDC motor reaches 700 RPM at the start of the robot's movement and the speed will start to drop to 0 when the robot approaches the predetermined point. The speed response using a BLDC motor is also very good because there is no oscillation and it is very stable. Figure 7(b) shows how steady the BLDC motor's reaction to steering is. It is proven that there is no oscillation and when the robot has approached the predetermined facing direction the steering angle will start to stabilize and keep the steering angle from changing until it reaches the desired facing direction. In terms of the performance, when the robot uses a BLDC motor, the robot runs quickly, accurately, and stably. Meanwhile, when the robot uses a DC motor, it runs fast but not accurate and unstable.
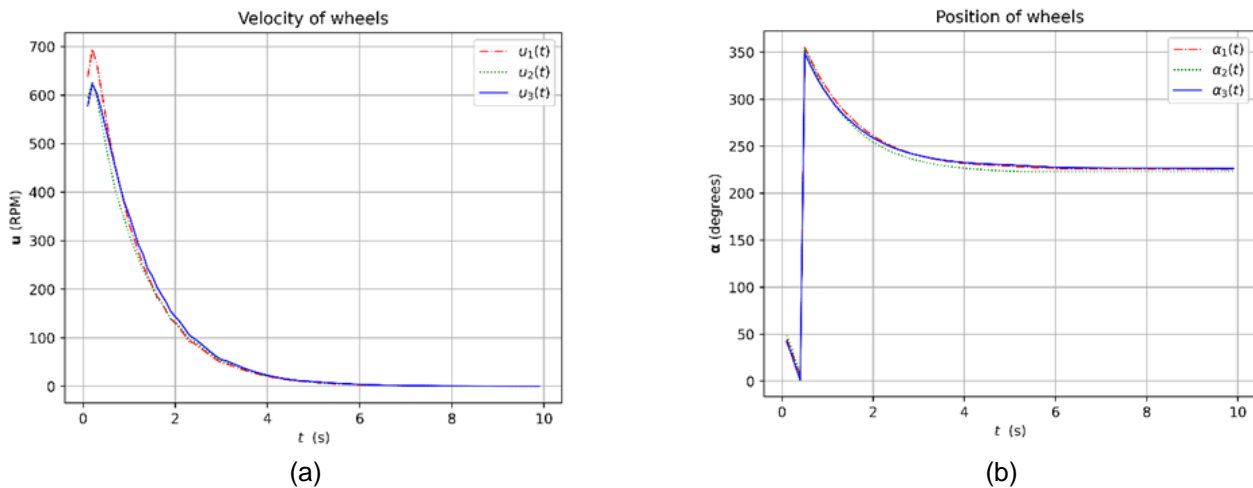

(a)   (b)

Figure 7. (a) Speed of Each Wheel using BLDC Motor, (b) Position of Each Wheel using BLDC Motor

3.2 Simulation kinematic of 3-wheels swerve drive using DC motor

The robot has moved successfully from the starting location (green arrow direction), which is (0,0), with facing 0°, to a predefined place (black arrow direction), which is (10,10), with facing 180°, as shown by Figure 8(a) and Figure 8(b). Even if everything is quiet, there is an oscillation, as seen by the trajectory traces (shown in gray) that are not inside the preset spot. The robot reaches a predetermined point very quickly which is evident in Figure 8(b) where the error value reaches 0 in the 4th second. Though the robot has accomplished its objectives, Figure 9(a) illustrates that the usage of a DC motor for driving indicates that the speed response of each wheel still cannot reach 0 RPM. This means that if the simulation time is extended, the robot will continue to move in oscillatory translation until it reaches its destination and the speed will be 0 RPM.
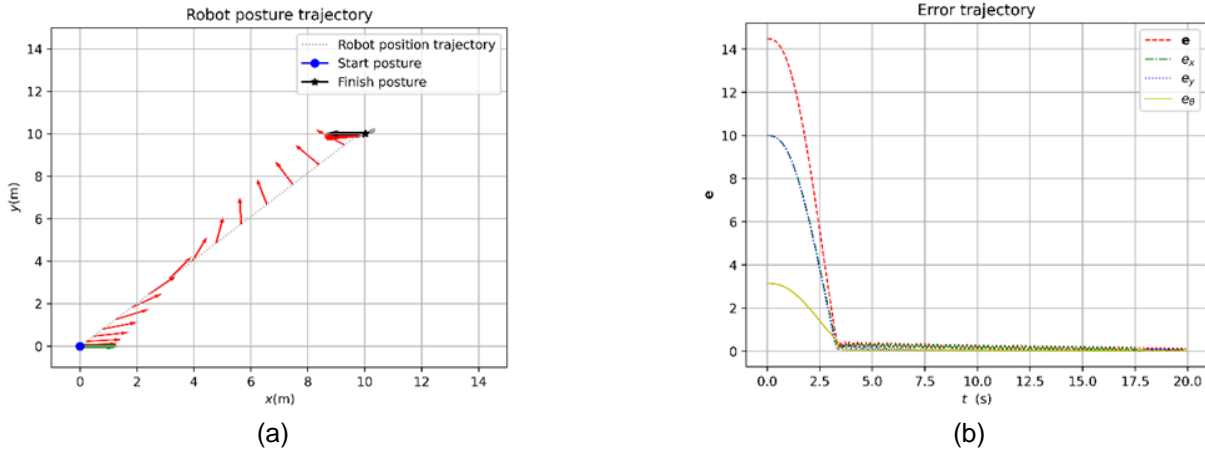
(a)   (b)

Figure 8. (a) Body Posture Robot using DC Motor, (b) Error Trajectory using DC Motor

Figure 9(b) illustrates how poorly a DC motor works for steering since the robot continues to move and oscillate while steering in the direction of the motor's destination. This means that if the driving wheel speed is still on, then the robot will move out of the destination point.
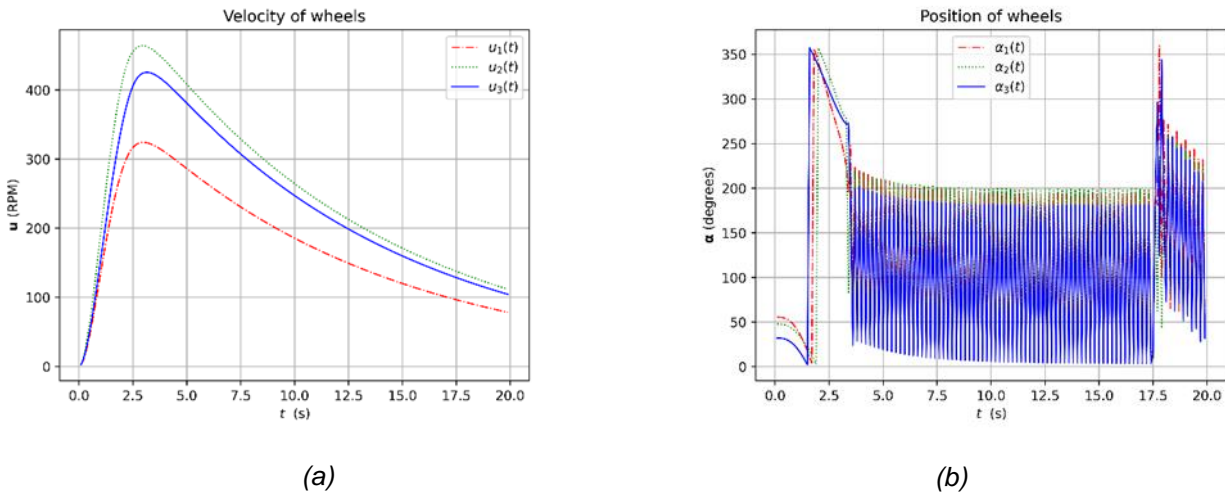

(a)   *(b)*

Figure 9. (a) Speed of Each Wheel using DC Motor, (b) Position of Each Wheel using DC Motor

4. Conclusion

In this study, the kinematic modeling simulation went very well, it was proven that the robot could go to the destination point correctly. The use of BLDC motors in driving and steering on swerve drive robots is better, more stable, and faster than using DC motors even though it reaches an error value of 0 within 5 seconds. When utilizing a DC motor, the robot's performance is not very good, especially in the steering part. In the steering part, there is still oscillation. Therefore, the solution to improve the robot's performance is to use a BLDC motor because by using a BLDC motor, the steering part does not experience oscillations. The BLDC motor not only improves the steering performance but also the driving performance. When using a DC motor, the maximum speed is only 450 RPM while when using a BLDC motor the maximum speed is 700 RPM. This is very good because it makes the robot move quickly and accurately according to the predetermined point. For further research, it is hoped that there will be additional sensors such as IMU and external encoder so that the direction is more precise and the robot can go to the destination point accurately. BLDC motor controllers such as the use of FOC also need to be added so that BLDC motors are more optimal.

References

[1]   D. Rijalusalam and I. Iswanto, "Implementation Kinematics Modeling and Odometry of Four Omni Wheel Mobile Robot on The Trajectory Planning and Motion Control Based Microcontroller," *Journal of Robotics and Control (JRC)*, vol. 2, Jan. 2021. https://doi.org/10.18196/jrc.25121

[2]   S. Rossi, M. Staffa, and A. Tamburro, "Correction to: Socially Assistive Robot for Providing Recommendations: Comparing a Humanoid Robot with a Mobile Application," *Int J Soc Robot*, vol. 11, p. 1, Jan. 2019. https://doi.org/10.1007/s12369-018-0489-0

[3]   N. Ghobadi and S. F. Dehkordi, "Dynamic modeling and sliding mode control of a wheeled mobile robot assuming lateral and longitudinal slip of wheels," in *2019 7th International Conference on Robotics and Mechatronics (ICRoM)*, Nov. 2019, pp. 150–155. https://doi.org/10.1109/ICRoM48714.2019.9071913

[4]   A. Sofwan, H. R. Mulyana, H. Afrisal, and A. Goni, "Development of Omni-Wheeled Mobile Robot Based-on Inverse Kinematics and Odometry," in *2019 6th International Conference on Information Technology, Computer and Electrical Engineering (ICITACEE)*, 2019, pp. 1–6. https://doi.org/10.1109/ICITACEE.2019.8904418

[5]   I. Reguii, I. Hassani, and C. Rekik, "Mobile Robot Navigation Using Planning Algorithm and Sliding Mode Control in a Cluttered Environment," *Journal of Robotics and Control (JRC)*, vol. 3, no. 2, pp. 166–175, 2022. https://doi.org/10.18196/jrc.v3i2.13765

[6]   D. and B. F. and P. J. I. Yunardi Riky Tri and Arifianto, "Holonomic implementation of three wheels omnidirectional mobile robot using DC motors," *Journal of Robotics and Control (JRC)*, vol. 2, pp. 65–71, 2021. https://doi.org/10.18196/jrc.2254

[7]   H. Taheri and C. X. Zhao, "Omnidirectional mobile robots, mechanisms and navigation approaches," *Mech Mach Theory*, vol. 153, p. 103958, 2020. https://doi.org/10.1016/j.mechmachtheory.2020.103958

[8]   M. Achmadiah, A. Rosyidin, A. Pracoyo, I. Siradjuddin, D. Permatasari, and G. Azhar, "Desain permodelan dan simulasi Field Oriented Control (FOC) menggunakan motor BLDC: Aplikasi pada Drive Train - Swerve Drive," *Jurnal Elektronika dan Otomasi Industri*, vol. 10, pp. 361–368, Jun. 2023. https://doi.org/10.33795/elkolind.v10i3.4416

[9]   X. Zhang, Y. Xie, L. Jiang, G. Li, J. Meng, and Y. Huang, "Trajectory Tracking of a 4wis4wid Robot Using Adaptive Receding Horizon Control Based on Neurodynamics Optimization," in *2019 ASME International Conference on Advanced Intelligent Mechatronics (AIM)*, 2019, pp. 565–570. https://doi.org/10.1109/AIM.2019.8868381

[10] I. Hassani, I. Maalej, and C. Rekik, "Backstepping tracking control for nonholonomic mobile robot," in *2020 4th International Conference on Advanced Systems and Emergent Technologies (ICASET)*, 2020, pp. 63–68. https://doi.org/10.1109/IC_ASET49463.2020.9318221

[11] P. Lin, D. Liu, D. Yang, Q. Zou, Y. Du, and M. Cong, "Calibration for Odometry of Omnidirectional Mobile Robots Based on Kinematic Correction," in *2019 14th International Conference on Computer Science I& Education (ICCSE)*, 2019, pp. 139–144. https://doi.org/10.1109/ICCSE.2019.8845402

[12] C. Wang, X. Liu, X. Yang, F. Hu, A. Jiang, and C. Yang, "Trajectory Tracking of an Omni-Directional Wheeled Mobile Robot Using a Model Predictive Control Strategy," *Applied Sciences*, vol. 8, p. 231, Feb. 2018. https://doi.org/10.3390/app8020231

[13] H. Ye, D. Wang, J. Wu, Y. Yue, and Y. Zhou, "Forward and inverse kinematics of a 5-DOF hybrid robot for composite material machining," *Robot Comput Integr Manuf*, vol. 65, p. 101961, 2020. https://doi.org/10.1016/j.rcim.2020.101961

[14] V. N. Kadam, L. Vachhani, and A. Gupta, "Control of an Omnidirectional Mobile Base with Multiple Spherical Robots," in *2019 Sixth Indian Control Conference (ICC)*, 2019, pp. 350–355. https://doi.org/10.1109/ICC47138.2019.9123198

[15] T. Dewi, S. Nurmaini, P. Risma, Y. Oktarina, and M. Roriz, "Inverse kinematic analysis of 4 DOF pick and place arm robot manipulator using fuzzy logic controller," *International Journal of Electrical and Computer Engineering (IJECE)*, vol. 10, pp. 1376–1386, Apr. 2020. https://doi.org/10.11591/ijece.v10i2.pp1376-1386

[16] M. Shamseldin, "Optimal Covid-19 Based PD/PID Cascaded Tracking Control for Robot Arm driven by BLDC Motor," *WSEAS Transactions on Systems*, vol. 20, pp. 217–227, Aug. 2021. https://doi.org/10.37394/23202.2021.20.24

[17] M. Dasari, S. A, and M. Kumar, "Modeling of a commercial BLDC motor and control using GA-ANFIS tuned PID controller," in *2017 International Conference on Innovative Research In Electrical Sciences (IICIRES)*, Jun. 2017, pp. 1–6. https://doi.org/10.1109/IICIRES.2017.8078305

[18] D. Mohanraj *et al.*, "A Review of BLDC Motor: State of Art, Advanced Control Techniques, and Applications," *IEEE Access*, vol. 10, pp. 54833–54869, 2022. https://doi.org/10.1109/ACCESS.2022.3175011

[19] M. Mary *et al.*, "Fuzzy PI Control of Trapezoidal Back EMF Brushless DC Motor Drive Based on the Position Control Optimization Technique," *Math Probl Eng*, vol. 2022, pp. 1–14, Jul. 2022. https://doi.org/10.1155/2022/4605449

[20] S. Nahar, Md. R. Ahmed, and Md. A. Rahman, "Performance Analysis of BLDC Motor using an Improved Methodology," in *2020 IEEE Region 10 Symposium (TENSYMP)*, 2020, pp. 586–589. https://doi.org/10.1109/TENSYMP50017.2020.9231024

[21] M. Mahmud, M. R. Islam, S. M. A. Motakabber, M. D. A. Satter, K. E. Afroz, and A. K. M. Ahasan Habib, "Control Speed of BLDC Motor using PID," in *2022 IEEE 18th International Colloquium on Signal Processing & Applications (CSPA)*, 2022, pp. 150–154. https://doi.org/10.1109/CSPA55076.2022.9782030

[22] H. Chang, S. Wang, and P. Sun, "Omniwheel Touchdown Characteristics and Adaptive Saturated Control for a Human Support Robot," *IEEE Access*, vol. 6, pp. 51174–51186, 2018. https://doi.org/10.1109/ACCESS.2018.2869836

[23] X. Liu *et al.*, "MPC-based high-speed trajectory tracking for 4WIS robot," *ISA Trans*, vol. 123, pp. 413–424, Feb. 2022. https://doi.org/10.1016/j.isatra.2021.05.018

[24] E. M. Ijaabo, A. Alsharkawi, and A. R. Firdaus, "Trajectory Tracking of an Omnidirectional Mobile Robot Using Sliding Mode Control," in *2019 2nd International Conference on Applied Engineering (ICAE)*, 2019, pp. 1–6. https://doi.org/10.1109/ICAE47758.2019.9221818

[25] Y. Luan, H. Wang, X. Li, W. Xu, R. Huang, and J. Lv, "Design of Motion Control System for Omnidirectional Four-Drive Mobile Robot," in *2019 IEEE 8th Joint International Information Technology and Artificial Intelligence Conference (ITAIC)*, 2019, pp. 1409–1413. https://doi.org/10.1109/ITAIC.2019.8785450

[26] K. Vanchinathan, K. R. Valluvan, C. Gnanavel, and C. Gokul, "Design Methodology and Experimental Verification of Intelligent Speed Controllers for Sensorless Permanent Magnet Brushless DC Motor," *International Transactions on Electrical Energy Systems*, Jun. 2021. https://doi.org/10.1002/2050-7038.12991

[27] M. Kelek, I. Çelik, U. Fidan, and Y. Oğuz, "The Simulation of Mathematical Model of Outer Rotor BLDC Motor," in *4th International Symposium on Innovative Approaches in Engineering and Natural Sciences, Samsun, Turkey*, Nov. 2019. https://doi.org/10.36287/setsci.4.6.106

[28] S. Trefilov, "Non-linear discrete model of BLDC motor for studying the range of permissible values of the voltage vector in the state space," *MATEC Web of Conferences*, vol. 329, p. 3070, Jan. 2020. https://doi.org/10.1051/matecconf/202032903070

[29] B. Hekimoğlu, "Optimal Tuning of Fractional Order PID Controller for DC Motor Speed Control via Chaotic Atom Search Optimization Algorithm," *IEEE Access*, vol. 7, pp. 38100–38114, 2019. https://doi.org/10.1109/ACCESS.2019.2905961